Epithelial and neutrophil interactions and coordinated response to *Shigella* in a human intestinal enteroid-neutrophil co-culture model

Jose M. Lemme-Dumit,[1] Michele Doucet,[2] Nicholas C. Zachos,[2]* and Marcela F. Pasetti[1,3]*

[1]Department of Pediatrics, Center for Vaccine Development and Global Health, University of Maryland School of Medicine, Baltimore, MD, USA.

[2]Department of Medicine, Division of Gastroenterology and Hepatology, Johns Hopkins University School of Medicine, Baltimore, MD, USA.

[3]Lead contact

*Corresponding authors:

Marcela F. Pasetti, Ph.D.
685 West Baltimore St.; HSF-I Room 480
Baltimore, MD 21201
Email: mpasetti@som.umaryland.edu
Phone: 410-706-2341; Fax: 410-706-6205

Nicholas C. Zachos, Ph.D.
720 Rutland Avenue; Ross Research Building Room 943
Baltimore, MD 21205
Email: nzachos1@jhmi.edu
Phone: 410-614-0128; Fax: 410-955-9677

Abstract

Polymorphonuclear neutrophils (PMN) are recruited to the gastrointestinal mucosa in response to infection. Herein, we report the development and the characterization of an *ex vivo* tissue co-culture model consisting of human intestinal enteroid monolayers and PMN, and a mechanistic interrogation of PMN-epithelial cell interaction and response to *Shigella,* a primary cause of childhood dysentery. Co-culture integration, barrier function, PMN phenotypic and functional attributes, and innate immune responses were examined. PMN within the enteroid monolayers acquired a distinct activated/migratory phenotype that was influenced by direct epithelial cell contact as well as by molecular signals. Seeded on the basal side of the intestinal monolayer, PMN intercalated within the epithelial cells and moved paracellularly toward the apical side. Co-cultured PMN also increased basal secretion of IL-8. *Shigella* added to the apical surface of the monolayers evoked additional PMN phenotypic adaptations, including increased expression of cell surface markers associated with chemotaxis and cell degranulation (CD47, CD66b and CD88). *Shigella* infection triggered rapid transmigration of PMN to the luminal side of monolayers resulting in phagocytosis and killing of organisms. *Shigella* infection modulated cytokine production in the co-culture; apical MCP-1, TNF-α, and basolateral IL-8 production were downregulated, while basolateral IL-6 secretion was increased. We demonstrate, for the first time, PMN phenotypic adaptation, mobilization, and coordinated epithelial cell-PMN innate response upon *Shigella* infection in the human intestinal environment. The epithelial cell-PMN co-culture represents a technical innovation for mechanistic interrogation of gastrointestinal physiology, host-microbe interaction, innate immunity, and evaluation of preventive/therapeutic tools.

Importance

Studies of mucosal immunity and microbial host cell interaction have traditionally relied on animal models and *in vitro* tissue culture using immortalized cancer cell lines, which render non-

physiological and often unreliable results. Herein we report the development and characterization of an *ex vivo* enteroid-PMN co-culture consisting of normal human intestinal epithelium and a mechanistic interrogation of PMN and epithelial cell interaction and function in the context of *Shigella* infection. We demonstrated tissue-driven phenotypic and functional adaptation of PMN and a coordinated epithelial cell and PMN response to *Shigella*, a primary cause of dysentery in young children in the developing world.

Introduction

The intestinal epithelium creates a physical and molecular barrier that protects the host from potentially damaging elements in the constantly changing outside environment. Epithelial barrier function is supported by a diverse population of underlying immune cells, which deploy a variety of host-defense mechanisms against harmful agents (1). Coordinated signals resulting from microbial sensing, cell-to-cell contact, cytokines, and other chemical mediators determine the type and extent of responses of gut immune cells, balancing tissue homeostasis with effective anti-microbial function via inflammation.

Advances in understanding intestinal physiology, pathophysiology, and host immunity have traditionally relied on studies conducted in animal models (or animal tissue) and in traditional tissue culture systems using colon cancer cell lines. Animal models, including the use of mutant mouse strains, have contributed to the mechanistic understanding of the composition, function, regulatory processes, and operatives of immunity at the gut mucosa. Unfortunately, host restrictions limit the utility and value of animal models (2, 3). This is the case for many enteric pathogens for which small animals fail to recreate disease as it occurs in humans. Likewise, immortalized (transformed) cell lines (e.g., HT-29, Caco-2, and T84) do not reflect human physiological responses but rather the aberrant behavior of diseased cells (e.g., karyotype defects). These cell-line based cultures also lack the multicellular complexity of the human intestinal epithelium, which further reduces the reliability and significance of the data generated.

The establishment of human enteroids from Lgr5^{+} intestinal stem cells was a breakthrough in tissue culture technology (4). Since then, three-dimensional (3D) intestinal enteroids have been widely used as models to study human gut physiology and pathophysiology as well as host-microbe interactions (5-7). Not only do enteroids render a truer physiological representation of the human epithelium, but they also offer a practical and reliable system to probe mechanisms and interventions at the gut mucosal interface. The 3D spheroid conformation can be adapted to produce a 2D monolayer configuration with enteroids seeded on a semipermeable membrane

(i.e., Transwell insert) (8-10). An important practical advantage to this simplified format is that it allows for direct and controlled access to the apical (mimicking the lumen) and basolateral side of the epithelial cells, thus facilitating experimental manipulation and evaluation of outcomes. Enteroid monolayers, which can be generated from any gut segment, can mimic the undifferentiated (crypt-like) and differentiated (villus-like) profile of the intestinal epithelial cells (i.e., absorptive enterocytes, goblet cells, enteroendocrine cells, and Paneth cells) (11) and display segment-specific phenotypic and functional attributes of the normal human gut (12). To better recreate the cellular complexity of the gastrointestinal mucosal barrier, we devised a human primary cell co-culture system consisting of enteroid monolayers and macrophages seeded on the basolateral side (11). Studies using this enteroid-macrophage co-culture model demonstrated physical and cytokine/chemokine-mediated interactions between intestinal epithelial cells and macrophages in the presence of pathogenic *E. coli* (11, 13). Aiming to expand this co-culture conformation to include other phagocytic cells, we established an *ex vivo* co-culture model containing intestinal epithelial cells and human primary polymorphonuclear neutrophils (PMN) facing the monolayers' basal membrane. The histological and functional features of this co-culture model, such as cell integration, PMN phenotype, PMN-epithelial cell physical and molecular interactions, and cell function were characterized. Coordinated epithelial and PMN anti-microbial response was examined using *Shigella* as model enteric pathogen. *Shigella* causes diarrhea and dysentery in humans by trespassing the colonic barrier via M cells and infecting epithelial cells, and this process involves massive recruitment of PMN (14). The enteroid-PMN co-culture modeled the paradoxical role of PMN contributing to inflammation and controlling infection.

Results

Establishment of a PMN-enteroid co-culture and PMN-epithelial cell interaction. To interrogate PMN adaptation and function in the human gut, we established an enteroid-PMN co-

culture model that contains human enteroid monolayers and peripheral blood isolated human PMN. A human enteroid-macrophage co-culture with similar configuration has been developed by our group (11). Human ileal 3D organoids derived from $Lgr5^{+}$-containing biopsies from healthy subjects were seeded upon the inner (upper) surface of a Transwell insert and allowed to grow until they reached confluency. PMN isolated from peripheral blood of healthy human adult volunteers and exhibiting a $CD15^{+}CD16^{+}CD14^{-}$ phenotype (15) were seeded on the outer (bottom) surface of the insert (Figure 1A). Confocal immunofluorescence microscopy and H&E staining confirmed the co-culture's expected epithelial cell polarity with the brush border oriented towards the luminal side (apical compartment) and adherent PMN facing the basolateral side of the monolayer (Figure 1B). Interestingly, PMN rapidly mobilized from the bottom side of the insert (where they were seeded) towards the epithelium. Within 2h of being added to the monolayers, PMN migrated from the insert and through the insert's pores (Figure S1) and intercalated within the epithelial cells (Figures 1B, C). The migrating PMN could be retrieved and enumerated in the apical compartment media (Figure 1D). The addition of PMN to the enteroid monolayer increased epithelial permeability, as shown by reduction in transepithelial electrical resistance (TER); although the difference did not reach statistical significance (Figure 1E). Because human IL-8 promotes PMN recruitment (16), we examined the effect of exogenous IL-8 on the mobilization of PMN co-cultured with epithelial cells and on monolayer permeability. Apical treatment of monolayers with 100 ng/ml IL-8 increased PMN epithelial transmigration (1.8-fold) (Figure 1D) and barrier permeability; the PMN-induced decrease in TER became statistically significant in the presence of IL-8 (Figure 1F). Importantly, IL-8 alone did not affect the permeability of monolayers (Figure 1F).

Since cell movement is influenced by molecular mediators, we next examined the presence of cytokines (pro- and anti-inflammatory) and chemoattractant molecules in tissue culture media collected from the apical and basolateral compartments of enteroid monolayers alone and of enteroid-PMN co-cultures. Basolateral levels of IL-8 produced by the PMN-containing enteroids

were 10-fold higher as compared to IL-8 produced by the monolayers alone, while MCP-1 and TNF-α remained unaffected by addition of PMN (Figure 1G). Similarly, the presence of PMN did not affect apical secretion of MCP-1, TNF-α, and IL-8 (Figure 1G). Production of MCP-1 was distinctly polarized, with higher levels being released to the apical side of the epithelial barrier. IL-1β, IL-6, IL-10, IL-12p70, IFN-γ, and TGF-β1 were measured but determined to be below the limit of detection of the assay for each cytokine.

Taken together, these results demonstrate adequate engraftment of PMN on the basolateral side of the enteroid monolayer, rapid migration of PMN across the monolayer to the luminal side, PMN-induced basolateral secretion of IL-8, and membrane de-stabilization (increased permeability) by IL-8-enhanced PMN transepithelial movement.

The human intestinal epithelium environment determines PMN immune phenotype and functional capacity. Cell phenotype, morphology, and function can be affected by the surrounding tissue and molecular environment. We hypothesized that the immune phenotype and functional capacity of PMN added to the enteroid monolayer would be influenced by their proximity or direct contact with the intestinal epithelium. To explore this hypothesis, we determined the expression of cell surface markers and phenotypic features of PMN isolated from peripheral blood in comparison with those of PMN within the enteroid co-culture. Two populations of co-cultured PMN were investigated following 2h of incubation: PMN residing within the monolayer and in direct contact with the epithelial cells and PMN harvested from the basolateral media as tissue adjacent milieu (Figure 2A). PMN co-cultured with enteroid monolayers had a distinct phenotypic profile as compared with PMN obtained from peripheral blood. Regardless of their location, PMN co-cultured with enteroid monolayers exhibited increased expression of CD18 (β2 integrin), a molecule that participates in extravasation of circulating PMN, as well as upregulation of CD47, a receptor for membrane integrins involved in

cell adhesion and migration, and of CD88 (C5a receptor), a molecule that mediates chemotaxis, granule enzyme release, and super anion production (Figure 2B; Figure S2B). CD66b, a marker of secondary granule exocytosis was likewise increased, but only in PMN harvested from the basolateral media (not in contact with cells) (Figure 2C; Figure S2B). In contrast, expression of CD182 (CXCR2 or IL-8RB) was reduced in all PMN added to co-culture, without distinction of retrieving site (Figure 2C; Figure S2B). PMN residing in close contact with epithelial cells exhibited increased expression of CD15 (E-selectin), a molecule that mediates PMN extravasation; CD16 (FcγRIII), a receptor for IgG that mediates degranulation, phagocytosis, and oxidative burst; and CD11b (α integrin), a protein that facilitates PMN adhesion and, along with CD18, forms the Mac-1 complex implicated in multiple anti-microbial functions (e.g., phagocytosis, cell-mediated cytotoxicity, cellular activation) (Figure 2D; Figure S2B). These results demonstrate that PMN within the intestinal epithelial environment undergo unique phenotypic adaptations, some of which are driven by molecular signals while others require direct PMN-epithelial cell contact.

PMN interaction with *Shigella* as a model enteric pathogen. To interrogate human epithelial cell and PMN interactions in the context of an enteric infection, we exposed the co-culture to wild type *Shigella flexneri* 2a (strain 2457T) as a model pathogen. PMN participate in *Shigella* pathogenesis through secretion of pro-inflammatory cytokines and deploy anti-microbial functions including phagocytosis, proteolytic enzymes, anti-microbial proteins, and neutrophil extracellular traps (NETs) production. We first determined baseline responses of peripheral blood PMN in the presence of *Shigella*. PMN phagocytosed FITC-labeled *S. flexneri* 2a 2457T within 10 min of exposure; bacterial phagocytosis increased over time (up to 1h tested) reaching a maximum effect at 30 min (Figure 3A). In parallel, the number of bacteria recovered from the culture supernatant of *Shigella*-exposed PMN decreased significantly within 30- and 60-min

exposure, in comparison to the number of bacteria recovered from control wells containing *Shigella* alone (in the absence of PMN) resuspended in tissue culture media or media that had been exposed to PMN to control for any soluble bactericidal source (Figure 3B). PMN viability was not affected during the first 2h of *Shigella* exposure, but decreased significantly by 3h post infection (Figure 3C). *Shigella*-exposed PMN exhibited changes in cell morphology and motility; formation of pseudopodia (projections of the cell membrane that enable locomotion) was observed within 30 min post infection (Figure 3D). In the presence of *Shigella*, PMN also displayed dynamic amoeboid motility toward the bacteria, and released NETs evidenced by a thick, diffuse, and opaque weave of DNA and entrapped bacilli (Figure 3E). FITC-stained *Shigella* colocalized with PMN phagolysosome (Figure 3F). In addition, PMN upregulated production and secretion of IL-8 and IL-1β, which are key molecular mediators of *Shigella* pathogenesis, 2h post infection, while production of IL-6 and MCP-1 was downregulated; production of TNF-α was not affected (Figure 3G). IL-10, TGF-β1, and IFN-γ were also measured but were below the limit of detection of the assay. A principal component analysis (PCA) of PMN function, viability, and cytokine production revealed an association between PMN-mediated phagocytosis and bactericidal activity with IL-8, IL-1β, and TNF-α production as indicated by principal component 1 on a PCA plot (Figure 3H). These results showed that PMN anti-microbial responses against *Shigella* involved morphological changes, phagocytic activity, and modulation of inflammatory cytokines.

Coordinated epithelial cell and PMN responses to *Shigella* in the co-culture model. We interrogated PMN and epithelial cell interactions and coordinated responses to *Shigella* in the PMN-enteroid co-cultures (Figure 1A). PMN were added to the enteroid monolayer as described above, allowed to settle for 2h, and then apically exposed to wild type *S. flexneri* 2a (MOI=10) for another 2h. Non-exposed co-cultures served as controls. Consistent with our previous

observation, PMN facing the basolateral side of the epithelial cells moved swiftly through the filter pores, traversed between the epithelial cells and across the monolayer, and protruded on the apical side. PMN basolateral-apical transmigration increased in the presence of *Shigella* (Figure 4A). PMN that traversed across the monolayer phagocytosed bacteria on the luminal surface as evidenced by confocal fluorescent microscopy (Figure 4B; $CD16^+$ PMN are stained in green, engulfed *S. flexneri* 2a in red; actin in white). The process created a hole in the otherwise confluent epithelium (Figure 4C). Addition of PMN to the enteroid monolayers enabled *Shigella* to reach the basolateral side, whereas in the absence of PMN, *Shigella* was unable to trespass the intact enteroid (Figure 4D). Reduced (1.3-fold) TER values were observed in the *Shigella*-exposed PMN-enteroid co-culture as compared with *Shigella*-exposed monolayers alone or the monolayer control (no PMN, no *Shigella*) (Figure 4E), consistent with loss of barrier function and tissue damage that allowed bacterial translocation.

We next examined cytokines produced by *Shigella*-infected and non-infected PMN-enteroid co-cultures. MCP-1, TNF-α, and IL-8 were detected in the apical and basolateral compartments, as described above. *Shigella* infection resulted in reduced apical production of MCP-1 and TNF-α by the co-cultured cells as well as in increased production of IL-6 and substantially reduced secretion of IL-8 basolaterally (Figure 4F). IL-6 was only detected in the infected cultures and exhibited a clear basolateral polarization (Figure 4F). Cultures were also tested for presence of IL-1β, which along with IL-8, are hallmarks of *Shigella* pathogenesis, but were not detectable. Collectively, these observations demonstrate that *Shigella* infection causes active recruitment of PMN to the luminal side, which results in discernible damage of the enteroid monolayer that paradoxically enables *Shigella* penetration and basolateral infection; still PMN actively engulfed bacteria and increased production and secretion of inflammatory cytokines to the apical and basolateral sides, respectively.

Phenotypic changes in PMN co-cultured with epithelial cells in response to *Shigella* infection. Additional experiments were conducted to determine the phenotypic features of PMN co-cultured with epithelial cells upon *Shigella* infection. PMN co-cultured with intestinal epithelial cells and exposed to *Shigella* exhibited increased expression of CD88, CD47, and CD66b as compared with PMN in co-cultures that remained uninfected (Figure 5A; Figure S3). In contrast, CD15 and CD18 expression was decreased on PMN from *Shigella*-infected co-cultures (Figure 5B; Figure S3). CD16, CD11b, and CD182 remained unchanged (Figure 5C; Figure S3). These results suggest that PMN residing within the intestinal environment undergo immune phenotypic adaptation as a result of pathogen exposure consistent with increased anti-microbial function (i.e., activation and expression of molecules that facilitate chemotaxis and epithelial transmigration).

Discussion

Epithelial cells and innate phagocytic cells underlying the intestinal epithelium work synergistically, preventing the trespassing of harmful agents and deploying rapid and effective host defense mechanisms against pathogens. PMN are the first innate immune cells recruited in response to gastrointestinal tissue inflammation and infection and they play a critical role initiating host immune responses (17). Patients with neutrophil disorders are prone to recurrent microbial infection (18, 19). We report in this manuscript the successful establishment of an *ex vivo* primary human intestinal epithelial-PMN co-culture and results from a mechanistic interrogation of cell interactions and innate responses to *Shigella* as a relevant diarrhoeagenic pathogen.

Our group developed the first *ex vivo* human enteroid- and monocyte-derived macrophage co-culture model in a monolayer format (11). The same approach was used to produce the PMN-enteroid co-culture described herein. Differently from macrophages, which remained in the basolateral side of the monolayer (where seeded) and responded to luminal

organisms by extending transepithelial projections between adjacent epithelial cells, PMN rapidly migrated from the basolateral side of the epithelial cell and across the monolayer via the paracellular space. Histological and confocal microscopy images revealed PMN crawling through the Transwell insert pores, embedding at the base of the epithelial cells, and emerging on the luminal side of the enteroid monolayer, all within a few hours of co-culture. While macrophages contributed to cell differentiation and stabilized the epithelial barrier in our previous studies, PMN transmigration resulted in increased barrier permeability that enabled bacteria invasion. Intestinal epithelial repair events (e.g., cell proliferation and migration, and closure of leaking epithelial lateral spaces) reportedly begin minutes after acute mucosal barrier injury (20). As a corollary of these observations, we are investigating epithelial repair subsequent to PMN-induced inflammation and cell disruption, and the mechanisms and elements involved.

The capacity of PMN to migrate across the vascular endothelium (21) and a variety of tissues (22, 23), including epithelial cell layers (24-27) has been documented *in vivo* (mainly in animal models) or *in vitro* using cell lines. These processes have been associated with PMN activation as a result of microbial sensing, inflammation, or danger signals. The level of myeloperoxidase (MPO), one of the principal enzymes contained in PMN granules and released upon activation, in stool is, in fact, a biomarker of inflammatory bowel disease severity (28). In our human PMN and intestinal epithelial cell co-culture model, PMN migrated even in the absence of external stimulatory signals. PMN are not typically present in the homeostatic gut but actively recruited by signs of inflammation or infection (29); therefore, unprovoked PMN migration would not be expected. From the technical standpoint, the 3.0 μm pore size Transwell membrane used in our model allowed not only for successful and consistent growth of enteroid monolayers, but also the basolateral-to-apical migration of PMN; this system is more practical than the traditional growing of epithelial cells in an inverted manner, typically used for cancer cell lines.

The tissue microenvironment can influence immune cell phenotype and effector function capabilities (30, 31). PMN from peripheral blood exhibited rapid phenotypic changes when incubated with enteroid monolayers. They acquired an activated phenotype that was triggered by tissue-derived signals. Compared to the PMN from peripheral blood, PMN co-cultured with epithelial cells had increased expression of CD18, which favors cell binding, of CD88, which is the receptor for C5a and facilitates degranulation and chemotaxis, and of CD47, a cell surface glycoprotein that supports transmigration across endothelial and epithelial cells (32-34). PMN phenotypic changes were influenced by their spatial location, i.e., whether they were in direct contact with epithelial cells or simply present in basolateral culture media. PMN in close proximity with the epithelium (the migratory PMN) had upregulated expression of CD15, which participates in chemotaxis and extravasation from circulation, as well as FcγRIII (CD16), a low affinity Fc receptor for IgG, and CD11b, a marker of cell adhesion and anti-microbial function (phagocytosis, degranulation, oxidative burst) (35, 36). On the other hand, PMN retrieved from the basolateral media, and which had not been in contact with the epithelial layer, exhibited increased expression of CD66b, indicative of PMN activation and degranulation (37). This is to our knowledge the first detailed description of dynamic changes of PMN immune phenotype in a translationally relevant model of the human intestinal epithelium.

MCP-1/CCL2, a chemoattractant and enhancer of bacterial killing and survival of phagocytic cells and IL-8, a potent promoter of PMN migration and tissue infiltration (38, 39), were abundantly produced by the ileal monolayers in our co-culture model. TNF-α, a recruiter and activator of phagocytic cells (40) was also detected, albeit at lower levels. IL-8, a hallmark product of intestinal epithelial cells, was further sourced by the PMN within the co-culture and released to the basolateral media; *in vivo* this subepithelial surge of IL-8 excess likely contributes to PMN recruitment. Expression of MCP-1, IL-8, and TNF-α has been reported in intestinal tissue of healthy adults in steady state (41, 42).

Again, when comparing PMN- and macrophage-enteroid co-cultures in terms of cytokine production, clear differences in innate immune functions emerged; while macrophages contributed to high levels of IFN-γ and IL-6, these cytokines were not detected in co-cultures containing PMN. The models were therefore capable of discerning morphological as well as functional cell adaptation.

Shigella invades the human colon and rectal mucosa and causes severe inflammation, massive recruitment of PMN, and tissue destruction (14). Bloody/mucous diarrhea (dysentery) with large numbers of PMN in stool are hallmarks of shigellosis (43).

Human intestinal enteroids can be infected with *Shigella* (44, 45). Hence, our model was fitting to interrogate coordinated innate responses of epithelial cells and PMN to this enteric pathogen. *Shigella* added on the luminal surface of the monolayers increased basolateral-apical PMN migration. Early efflux of PMN into the colonic tissue has been observed during shigellosis in the infected rabbit loop model (46). *Shigella*-induced PMN transmigration had been reported *in vitro* using colonic T84 cells (47). Sansonetti and colleagues had shown that *S. flexneri* lipopolysaccharide trancytosed to the basolateral side of T84 cells in the presence of human normal sera and enhanced adherence of subepithelial PMN through IL-8 signaling (48).

PMN transmigration across the intestinal monolayer in our co-culture model caused microscopically visible epithelial cell damage and created a conduit for bacterial invasion and possibly amplification of infection. This observation is consistent with focal breakdown of the epithelial cell surface attributed to PMN migration in various disease states including infectious enterocolitis (49). Our findings challenge for the first time the notion that M cells are necessary for *Shigella* epithelial translocation and invasion, and hint that the infiltration and barrier disruption by PMN offer another mechanism by which *Shigella* and other invasive enteric pathogens access the host internal compartment. We are presently studying reverse transmigration of bacteria-loaded PMN (out of the lumen and back to the basolateral side) as a possible means to initiate adaptive immunity through cross-presentation. The model lends itself

to study of molecules that reduce PMN activity in the context of enteric infections and could prevent intestinal injury and inflammation.

Although acting in a “brute force” manner, PMN deployed potent anti-microbial activity against *Shigella*. As expected, PMN from circulation phagocytosed *Shigella* rapidly and efficiently and entrapped bacteria into NET structures. PMN anti-microbial functions coincided with increased production of IL-8 and the pyroptosis-inducer IL-1β, and downregulation of IL-6 and MCP-1. Likewise, PMN embedded within the epithelial cells promptly mobilized upon sensing *Shigella* on the epithelial cell surface and exhibited robust phagocytic capacity. Intriguingly, IL-8 levels were reduced, IL-1β was absent, and IL-6 was increased in the infected PMN-epithelial co-culture as compared to non-infected. A reduction of IL-8 production had been reported in *Shigella*-infected human colonic explants, which was ascribed to anti-inflammatory bacterial proteins or death of IL-8 secreting cells (50). Reduced levels of these inflammatory cytokines may also reflect a regulatory feedback to prevent further tissue damage. Heightened levels of IL-6 and reduced TNF-α during infection may suggest a protective epithelial mechanism after injury (51, 52). In addition, IL-6 has been attributed a beneficial role in enhancing Th17-protective immunity against *Shigella* re-infection (53). Because cytokines measured in the co-culture supernatant represent the total amount produced by diverse cell types, this readout is limited in its capacity to discern subtle differences between culture conditions.

The immune phenotype of PMN in the co-culture adapted again as a result of *Shigella* infection, with further increases in activation/granule-associated markers CD66b, CD88, and CD47. CD47 has been implicated in PMN paracellular migration through epithelial cells in response to bacterium-derived leukocyte chemoattractant N-formyl-methionyl-leucyl-phenylalanine, in a process that involves intracellular distribution and increased CD47 cell surface expression (33). CD47-deficient mice have increased susceptibility to *E. coli* as a result

of reduced PMN trafficking and bacterial killing activity (54). This finding is consistent with our observed upregulation of CD47 in *Shigella*-exposed PMN, which is likely associated with PMN's anti-microbial activity. CD16 and CD11b expression were unaltered on PMN co-cultured with intestinal enteroids and exposed to *Shigella*, indicating a preserved phagocytic capacity, whereas extravasation and cell adhesion markers CD15 and CD18 were downregulated. It has been reported that CD47 expression increases gradually and modulates CD11b-integrin function and CD11b/CD18 surface expression on PMN, suggesting a regulatory mechanism between these molecules (33, 55). Expression of CD47 is self-protective; it avoids clearance by phagocytic cells (56). The exact role of CD47 expression on PMN during *Shigella* infection remains to be elucidated.

Human intestinal xenografts in immunodeficient mice have been used to model interactions of *Shigella* with the human intestine *in vivo*. The model failed to discern any role of PMN in ameliorating or exacerbating disease, but revealed larger intracellular bacteria in PMN-depleted mice; the authors conclude that while PMN may contribute to tissue damage, they are important in controlling bacteria dissemination. The combination of species, immunodeficient background, and impracticality are major confounders/limitations of this model (57).

Our studies provided new insights on the close communication between PMN and epithelial cells, phenotypic and functional changes on PMN prompted by the gastrointestinal environment, and their coordinated responses to *Shigella* as a model gastrointestinal pathogen. The PMN-epithelial cell co-culture described here provides a translationally relevant *ex vivo* model to study human epithelial cell-PMN physiology and pathophysiology, as well as host cell interactions and innate responses to enteric organisms. This model could be useful to interrogate innate immune defense mechanisms to enteric pathogens and to support the development and evaluation of preventive or therapeutic tools.

Materials and methods

Human PMN isolation

Human peripheral blood was collected in EDTA tubes (BD Vacutainer) from healthy volunteers enrolled in University of Maryland Institutional Review Board (IRB) approved protocol #HP-40025-CVD4000, and methods were conducted in compliance with approved Environmental Health and Safety guidelines (IBC #00003017). PMN were obtained by Ficoll-Paque (PREMIUM solution, GE Healthcare Bio-Sciences AB, Sweden) gradient centrifugation following dextran (Alfa Aesar, USA) sedimentation (58). Contaminating erythrocytes were removed by hypotonic lysis. After washing, cells (>95% of PMN determined by flow cytometry and May-Grünwald-Giemsa stained cytopreps) were suspended in enteroid differentiation media (DFM) without antibiotics and immediately used. Cell counting and viability were determined using Guava Viacount Flex Reagent (Luminex, USA) following the manufacturer's instruction and analyzed in Guava 8HT using Viacount software (Luminex, USA).

Tissue collection and enteroid generation

Human enteroid cultures were established from biopsy tissue obtained after endoscopic or surgical resection from healthy subjects at Johns Hopkins University under Johns Hopkins University IRB approved protocol #NA-00038329, as previously described (59). Briefly, enteroids generated from isolated intestinal crypts from ileal segments were maintained as cysts embedded in Matrigel (Corning, USA) in 24-well plates and cultured in Wnt3A containing non-differentiated media (NDM) (58). Multiple enteroid cultures were harvested with Culturex Organoid Harvesting Solution (Trevigen, USA), and small enteroid fragments were obtained by digestion with TrypLE Express (ThermoFisher) in 37°C water bath for 90 seconds. Enteroid fragments were resuspended in NDM containing 10 μM Y-27632 and 10 μM CHIR 99021 inhibitors (Tocris) (NDM+inhibitors). The inner surface of Transwell inserts (3.0 μm pore transparent polyester membrane) pre-coated with 100 μl of human collagen IV solution (34

392 μg/ml; Sigma-Aldrich, USA) were seeded with 100 μl of an enteroid fragment suspension, and
393 600 μl of NDM+inhibitors was added to the wells of a 24-well tissue culture plate and incubated
394 at 37°C, 5% CO_2, as previously described (58). NDM without inhibitors were replaced after 48h,
395 and fresh NDM was added every other day; under these conditions, enteroid cultures reached
396 confluency in 14-16 days. Monolayer differentiation was induced by incubation in Wnt3A-free
397 and Rspo-1-free DFM without antibiotics for 5 days (11). Monolayer confluency was monitored
398 by measuring TER values with an epithelial voltohmmeter (EVOM^2; World Precision
399 Instruments, USA). The unit area resistances (ohm*cm^2) were calculated according to the
400 growth surface area of the inserts (0.33 cm^2).
401
402 **PMN-enteroid co-culture**
403 Differentiated enteroid monolayers seeded on Transwell inserts were inverted and placed into
404 an empty 12-well plate. PMN (5x10^5 in 50 μl of DFM) were added onto the bottom surface of the
405 inserts and cells were allowed to attach for 2h at 37°C, 5% CO_2 (inserts remained wet
406 throughout this process). The inserts were then turned back to their original position into a 24-
407 well plate, and DFM was added to the insert (100 μl) and into the well (600 μl). Approximately
408 45% of the total PMN remained attached to the Transwell insert. TER measurements were
409 collected after 2h, allowing monolayer recovering.
410
411 ***Shigella flexneri* 2a infection**
412 *Shigella flexneri* 2a wild type strain 2457T was grown from frozen stocks (-80°C) on Tryptic Soy
413 Agar (TSA) (Difco BD, USA) supplemented with 0.01% Congo Red dye (Sigma-Aldrich)
414 overnight at 37°C. Bacterial inoculum was made by resuspending single red colonies in sterile
415 1X PBS pH 7.4 (Quality Biological). Bacterial suspension was adjusted to the desired
416 concentration (~1x10^8 CFU/ml) in advanced DMEM/F12 without serum. A bacterial suspension

containing ~ $5x10^6$ CFU in 50 µl was added directly to PMN (for 30-60 min) or to the apical compartment of enteroid monolayers alone or PMN-enteroid co-culture (for 2h), a multiplicity of infection of 10 relative to 1 PMN.

PMN transmigration

Basolateral-to-apical PMN transmigration was quantified by measurement of PMN MPO using a commercial kit (Cayman Chemical, Ann Arbor, MI) as previously described (60). The assay was standardized with a known number of human PMN. MPO activity in lysates of enteroid monolayer alone was negligible.

PMN phagocytosis

S. flexneri 2a cultures grown overnight as described above were washed, resuspended in sterile PBS and incubated with FITC (Sigma-Aldrich) (20 µg/ml) for 30 min at 37□C. The bacteria suspension was thoroughly washed and adjusted to ~10^8 CFU/ml in sterile PBS/glycerol (1:2), and stored at -80□C until used. The day of the assay, FITC-labeled *Shigella* was incubated with PMN-autologous human sera for 30 min at 37□C. Opsonized bacteria $5x10^6$ CFU was added to PMN suspension ($5x10^5$ cells) and incubated for 10, 30, and 60 min. Phagocytosis was measured by flow cytometry. External fluorescence was blocked with the addition of trypan blue, and the difference between MFI blocked and non-blocked samples was used to calculate % phagocytosis (61, 62).

H&E and immunofluorescence staining

PMN-enteroid co-culture cells were fixed in aqueous 4% paraformaldehyde (PFA; Electron Microscopy Sciences, USA) at room temperature (RT) for 45 min and then washed with PBS. For H&E staining, monolayers were kept for at least 48h in formaldehyde solution, then

embedded in paraffin, sectioned, mounted on slides, and stained with H&E. For immunofluorescence, cells were permeabilized and blocked for 30 min at RT in PBS containing 15% FBS, 2% BSA, and 0.1% saponin (all Sigma-Aldrich, USA). Cells were rinsed with PBS and incubated overnight at 4□C with primary antibodies: mouse anti-CD16 (LSBio, USA), rabbit anti-*S. flexneri* 2a (Abcam, USA) diluted 1:100 in PBS containing 15% FBS and 2% BSA. Stained cells were washed with PBS and incubated with secondary antibodies: goat anti-mouse AF488, goat anti-rabbit AF594 (all Thermo Fisher Scientific, USA) diluted 1:100 in PBS 1h at RT; phalloidin AF594 or AF633 (Molecular Probes, Thermo Fisher Scientific) was included in this step for actin visualization. Cells were washed and mounted in ProLong Gold Antifade Reagent with DAPI (Cell Signaling Technology, USA) for nuclear staining and maintained at 4□C. Lysosome was stained with LysoTracker™ Red DND-99 (Thermo Fischer Scientific) following the manufacturer's instructions.

Immunofluorescence microscopy

Confocal imaging was carried out at the Confocal Microscopy Facility of the University of Maryland School of Medicine using a Nikon W1 spinning disk confocal microscope running NIS-Elements imaging software (Nikon). Images were captured with a 40X or 60X oil objective and settings were adjusted to optimize signal. Immunofluorescence imaging (Figure 3F) was carried out using EVOS FL Imaging systems (fluorescent microscope) at 40X objective lens. Images were collated using FIJI/ImageJ (NIH). Signal processing was applied equally across the entire image. Actin channel was arranged to white-grey color for contrast purpose.

Flow cytometry

Cell phenotype was determined using the following human specific monoclonal antibodies from BD Pharmingen: HI98 (anti-CD15, FITC-conjugated), M5E2 (anti-CD14, APC-conjugated), 3G8 (anti-CD16, PE/Cy7-conjugated), D53-1473 (anti-CD88, BV421-conjugated), and BioLegend:

TS1/18 (anti-CD18, PE/Cy7-conjugated), ICRF44 (anti-CD11b, BV421-conjugated), 5E8/CXCR2 (anti-CD182, APC-conjugated), CC2C6 (anti-CD47, PE/Cy7-conjugated), HA58 (anti-CD54, APC-conjugated), G10F5 (anti-CD66b, Pacific Blue-conjugated). PMN were blocked with 2% normal mouse serum (Thermo Fisher Scientific) for 15 min at 4□C. After washing, cells were resuspended in FACS buffer (PBS containing 0.5% BSA and 2 mM EDTA; all Sigma-Aldrich) and 100 µl of equal number of cells were dispensed in several tubes and stained with antibodies for 30 min at 4□C. Antibodies were used diluted 1:2 – 1:1,000; optional amount was determined by in-house titration. Cells were washed in FACS buffer and either analyzed or fixed in 4% PFA for 15 min at 4□C and analyzed the next day. Marker expression was analyzed in a Guava 8HT using Guava ExpressPro software (Luminex, USA) or BD LSRII using FACSDiva software (BD Biosciences, USA) and analyzed with FlowJo software (v10, Tree Star).

Cytokine and chemokine measurements

Cytokines and chemokines were measured by electrochemiluminescence microarray using commercial assays (Meso Scale Diagnostic, USA) following the manufacturer's instructions. IFN-γ, IL-1β, IL-6, IL-10, IL-12p70, TNF-α, MCP-1, TGF-β1, and IL-8 were reported as total amount (pg) contained in the entire volume of apical (100 µl) and basolateral (600 µl) culture supernatants.

Statistical analysis

Statistical significances were calculated using the Student's *t*-test unpaired, one-way or two-way analysis of variance (ANOVA) with Tukey's post-test as appropriate. PCA was performed by selecting PC with eigenvalues greater than 1.0 (Kaiser rule). Plots and statistical tests were performed using Prism software v9 (GraphPad, San Diego, CA). Treatment comparisons

included at least three replicates and three independent experiments. Differences were considered statistically significant at *p*-value ≤ 0.05. Exact *p* values are indicated in each Figure. Results are expressed as mean ± standard error of mean (sem).

Acknowledgements

The authors want to thank Dr. Mark Donowitz, for critical reading of the manuscript and Robin Barnes and Nancy Greenberg, Clinical Research Nurses at University of Maryland, for their assistance in obtaining peripheral blood samples. The authors would like to acknowledge the Integrated Physiology Core of the Hopkins Conte Digestive Disease Basic and Translational Research Core Center (NIH P30 DK-089502 to N.C.Z.) for providing human enteroids and growth factor conditioned media and the University of Maryland School of Medicine Center for Innovative Biomedical Resources, Flow Cytometry Shared Service. This work was supported by NIH/NIAID P01AI125181 Immunology and Enteroid Cores, and 1R01AI117734-01 to M.F.P.

Author Contributions

J.M.L-D. designed and performed experiments, conducted data analyses and interpretation. M.D. provided initial assistance with enteroid monolayers. N.C.Z. and M.F.P. participated in experimental design, data analyses and interpretation, and supervised the study. J.M.L-D. and M.F.P. wrote the manuscript. All authors edited the manuscript.

Disclosures

The authors have no financial conflicts of interest.

References

1. Peterson LW, Artis D. 2014. Intestinal epithelial cells: regulators of barrier function and immune homeostasis. Nat Rev Immunol 14:141-53.
2. Mestas J, Hughes CC. 2004. Of mice and not men: differences between mouse and human immunology. J Immunol 172:2731-8.
3. Gibbons DL, Spencer J. 2011. Mouse and human intestinal immunity: same ballpark, different players; different rules, same score. Mucosal Immunol 4:148-57.
4. Barker N, van Es JH, Kuipers J, Kujala P, van den Born M, Cozijnsen M, Haegebarth A, Korving J, Begthel H, Peters PJ, Clevers H. 2007. Identification of stem cells in small intestine and colon by marker gene Lgr5. Nature 449:1003-7.
5. Zhang YG, Wu S, Xia Y, Sun J. 2014. Salmonella-infected crypt-derived intestinal organoid culture system for host-bacterial interactions. Physiol Rep 2:e12147.
6. Huang JY, Sweeney EG, Sigal M, Zhang HC, Remington SJ, Cantrell MA, Kuo CJ, Guillemin K, Amieva MR. 2015. Chemodetection and destruction of host urea allows Helicobacter pylori to locate the epithelium. Cell Host Microbe 18:147-56.
7. Co JY, Margalef-Catala M, Li X, Mah AT, Kuo CJ, Monack DM, Amieva MR. 2019. Controlling epithelial polarity: A human enteroid model for host-pathogen interactions. Cell Rep 26:2509-2520.e4.
8. Foulke-Abel J, In J, Kovbasnjuk O, Zachos NC, Ettayebi K, Blutt SE, Hyser JM, Zeng XL, Crawford SE, Broughman JR, Estes MK, Donowitz M. 2014. Human enteroids as an ex-vivo model of host-pathogen interactions in the gastrointestinal tract. Exp Biol Med (Maywood) 239:1124-34.
9. In J, Foulke-Abel J, Zachos NC, Hansen AM, Kaper JB, Bernstein HD, Halushka M, Blutt S, Estes MK, Donowitz M, Kovbasnjuk O. 2016. Enterohemorrhagic Escherichia coli reduce mucus and intermicrovillar bridges in human stem cell-derived colonoids. Cell Mol Gastroenterol Hepatol 2:48-62 e3.
10. Rajan A, Vela L, Zeng XL, Yu X, Shroyer N, Blutt SE, Poole NM, Carlin LG, Nataro JP, Estes MK, Okhuysen PC, Maresso AW. 2018. Novel segment- and host-specific patterns of Enteroaggregative Escherichia coli adherence to human intestinal enteroids. mBio 9:e02419-17.
11. Noel G, Baetz NW, Staab JF, Donowitz M, Kovbasnjuk O, Pasetti MF, Zachos NC. 2017. A primary human macrophage-enteroid co-culture model to investigate mucosal gut physiology and host-pathogen interactions. Sci Rep 7:45270.
12. In JG, Foulke-Abel J, Estes MK, Zachos NC, Kovbasnjuk O, Donowitz M. 2016. Human mini-guts: new insights into intestinal physiology and host-pathogen interactions. Nat Rev Gastroenterol Hepatol 13:633-642.
13. Noel G, Doucet M, Nataro JP, Kaper JB, Zachos NC, Pasetti MF. 2018. Enterotoxigenic Escherichia coli is phagocytosed by macrophages underlying villus-like intestinal epithelial cells: modeling ex vivo innate immune defenses of the human gut. Gut Microbes 9:382-389.
14. Sansonetti PJ, Arondel J, Cantey JR, Prevost MC, Huerre M. 1996. Infection of rabbit Peyer's patches by Shigella flexneri: effect of adhesive or invasive bacterial phenotypes on follicle-associated epithelium. Infect Immun 64:2752-64.
15. Gustafson MP, Lin Y, Maas ML, Van Keulen VP, Johnston PB, Peikert T, Gastineau DA, Dietz AB. 2015. A method for identification and analysis of non-overlapping myeloid immunophenotypes in humans. PLoS One 10:e0121546.
16. Metzemaekers M, Vandendriessche S, Berghmans N, Gouwy M, Proost P. 2020. Truncation of CXCL8 to CXCL8(9-77) enhances actin polymerization and in vivo migration of neutrophils. J Leukoc Biol 107:1167-1173.
17. Fournier BM, Parkos CA. 2012. The role of neutrophils during intestinal inflammation. Mucosal Immunol 5:354-66.

18. Lekstrom-Himes JA, Gallin JI. 2000. Immunodeficiency diseases caused by defects in phagocytes. N Engl J Med 343:1703-14.
19. Wortmann SB, Van Hove JLK, Derks TGJ, Chevalier N, Knight V, Koller A, Oussuren E, Mayr JA, van Spronsen FJ, Lagler FB, Gaughan S, Van Schaftingen E, Veiga-da-Cunha M. 2020. Treating neutropenia and neutrophil dysfunction in glycogen storage disease IB with an SGLT2-inhibitor. Blood doi:10.1182/blood.2019004465:2019004465.
20. Blikslager AT, Moeser AJ, Gookin JL, Jones SL, Odle J. 2007. Restoration of barrier function in injured intestinal mucosa. Physiol Rev 87:545-64.
21. Sullivan DP, Bui T, Muller WA, Butin-Israeli V, Sumagin R. 2018. In vivo imaging reveals unique neutrophil transendothelial migration patterns in inflamed intestines. Mucosal Immunol 11:1571-1581.
22. Lammermann T, Afonso PV, Angermann BR, Wang JM, Kastenmuller W, Parent CA, Germain RN. 2013. Neutrophil swarms require LTB4 and integrins at sites of cell death in vivo. Nature 498:371-5.
23. Uderhardt S, Martins AJ, Tsang JS, Lammermann T, Germain RN. 2019. Resident macrophages cloak tissue microlesions to prevent neutrophil-driven inflammatory damage. Cell 177:541-555 e17.
24. Sumagin R, Robin AZ, Nusrat A, Parkos CA. 2014. Transmigrated neutrophils in the intestinal lumen engage ICAM-1 to regulate the epithelial barrier and neutrophil recruitment. Mucosal Immunol 7:905-15.
25. Parkos CA, Delp C, Arnaout MA, Madara JL. 1991. Neutrophil migration across a cultured intestinal epithelium. Dependence on a CD11b/CD18-mediated event and enhanced efficiency in physiological direction. J Clin Invest 88:1605-12.
26. Brazil JC, Liu R, Sumagin R, Kolegraff KN, Nusrat A, Cummings RD, Parkos CA, Louis NA. 2013. alpha3/4 Fucosyltransferase 3-dependent synthesis of Sialyl Lewis A on CD44 variant containing exon 6 mediates polymorphonuclear leukocyte detachment from intestinal epithelium during transepithelial migration. J Immunol 191:4804-17.
27. Flemming S, Luissint AC, Nusrat A, Parkos CA. 2018. Analysis of leukocyte transepithelial migration using an in vivo murine colonic loop model. JCI Insight 3:e99722.
28. Masoodi I, Kochhar R, Dutta U, Vaishnavi C, Prasad KK, Vaiphei K, Hussain S, Singh K. 2012. Evaluation of fecal myeloperoxidase as a biomarker of disease activity and severity in ulcerative colitis. Dig Dis Sci 57:1336-40.
29. Kolaczkowska E, Kubes P. 2013. Neutrophil recruitment and function in health and inflammation. Nat Rev Immunol 13:159-75.
30. Grunwell JR, Giacalone VD, Stephenson S, Margaroli C, Dobosh BS, Brown MR, Fitzpatrick AM, Tirouvanziam R. 2019. Neutrophil dysfunction in the airways of children with acute respiratory failure due to lower respiratory tract viral and bacterial coinfections. Sci Rep 9:2874.
31. Svedberg FR, Brown SL, Krauss MZ, Campbell L, Sharpe C, Clausen M, Howell GJ, Clark H, Madsen J, Evans CM, Sutherland TE, Ivens AC, Thornton DJ, Grencis RK, Hussell T, Cunoosamy DM, Cook PC, MacDonald AS. 2019. The lung environment controls alveolar macrophage metabolism and responsiveness in type 2 inflammation. Nat Immunol 20:571-580.
32. Vainer B, Nielsen OH, Horn T. 2000. Comparative studies of the colonic in situ expression of intercellular adhesion molecules (ICAM-1, -2, and -3), beta2 integrins (LFA-1, Mac-1, and p150,95), and PECAM-1 in ulcerative colitis and Crohn's disease. Am J Surg Pathol 24:1115-24.
33. Liu Y, Merlin D, Burst SL, Pochet M, Madara JL, Parkos CA. 2001. The role of CD47 in neutrophil transmigration. Increased rate of migration correlates with increased cell surface expression of CD47. J Biol Chem 276:40156-66.

34. Parkos CA, Colgan SP, Liang TW, Nusrat A, Bacarra AE, Carnes DK, Madara JL. 1996. CD47 mediates post-adhesive events required for neutrophil migration across polarized intestinal epithelia. J Cell Biol 132:437-50.
35. Golay J, Valgardsdottir R, Musaraj G, Giupponi D, Spinelli O, Introna M. 2019. Human neutrophils express low levels of FcgammaRIIIA, which plays a role in PMN activation. Blood 133:1395-1405.
36. Teschner D, Cholaszczynska A, Ries F, Beckert H, Theobald M, Grabbe S, Radsak M, Bros M. 2019. CD11b regulates fungal outgrowth but not neutrophil recruitment in a mouse model of invasive pulmonary aspergillosis. Front Immunol 10:123.
37. Zhao L, Xu S, Fjaertoft G, Pauksen K, Hakansson L, Venge P. 2004. An enzyme-linked immunosorbent assay for human carcinoembryonic antigen-related cell adhesion molecule 8, a biological marker of granulocyte activities in vivo. J Immunol Methods 293:207-14.
38. Altstaedt J, Kirchner H, Rink L. 1996. Cytokine production of neutrophils is limited to interleukin-8. Immunology 89:563-8.
39. Andrews C, McLean MH, Durum SK. 2018. Cytokine tuning of intestinal epithelial function. Front Immunol 9:1270.
40. Ruder B, Atreya R, Becker C. 2019. Tumour necrosis factor alpha in intestinal homeostasis and gut related diseases. Int J Mol Sci 20.
41. Reinecker HC, Loh EY, Ringler DJ, Mehta A, Rombeau JL, MacDermott RP. 1995. Monocyte-chemoattractant protein 1 gene expression in intestinal epithelial cells and inflammatory bowel disease mucosa. Gastroenterology 108:40-50.
42. Raqib R, Lindberg AA, Wretlind B, Bardhan PK, Andersson U, Andersson J. 1995. Persistence of local cytokine production in shigellosis in acute and convalescent stages. Infect Immun 63:289-96.
43. Kotloff KL, Riddle MS, Platts-Mills JA, Pavlinac P, Zaidi AKM. 2018. Shigellosis. Lancet 391:801-812.
44. Ranganathan S, Doucet M, Grassel CL, Delaine-Elias B, Zachos NC, Barry EM. 2019. Evaluating Shigella flexneri pathogenesis in the human enteroid model. Infect Immun 87:e00740-18.
45. Koestler BJ, Ward CM, Fisher CR, Rajan A, Maresso AW, Payne SM. 2019. Human intestinal enteroids as a model system of Shigella pathogenesis. Infect Immun 87:e00733-18.
46. Perdomo OJ, Cavaillon JM, Huerre M, Ohayon H, Gounon P, Sansonetti PJ. 1994. Acute inflammation causes epithelial invasion and mucosal destruction in experimental shigellosis. J Exp Med 180:1307-19.
47. Perdomo JJ, Gounon P, Sansonetti PJ. 1994. Polymorphonuclear leukocyte transmigration promotes invasion of colonic epithelial monolayer by Shigella flexneri. J Clin Invest 93:633-43.
48. Beatty WL, Sansonetti PJ. 1997. Role of lipopolysaccharide in signaling to subepithelial polymorphonuclear leukocytes. Infect Immun 65:4395-404.
49. Yardley JH, Donowitz M. 1977. Colo-rectal biopsy in inflammatory bowel disease. Monogr Pathol:50-94.
50. Coron E, Flamant M, Aubert P, Wedel T, Pedron T, Letessier E, Galmiche JP, Sansonetti PJ, Neunlist M. 2009. Characterisation of early mucosal and neuronal lesions following Shigella flexneri infection in human colon. PLoS One 4:e4713.
51. Kuhn KA, Manieri NA, Liu TC, Stappenbeck TS. 2014. IL-6 stimulates intestinal epithelial proliferation and repair after injury. PLoS One 9:e114195.
52. Ye D, Ma I, Ma TY. 2006. Molecular mechanism of tumor necrosis factor-alpha modulation of intestinal epithelial tight junction barrier. Am J Physiol Gastrointest Liver Physiol 290:G496-504.

53. Sellge G, Magalhaes JG, Konradt C, Fritz JH, Salgado-Pabon W, Eberl G, Bandeira A, Di Santo JP, Sansonetti PJ, Phalipon A. 2010. Th17 cells are the dominant T cell subtype primed by Shigella flexneri mediating protective immunity. J Immunol 184:2076-85.
54. Lindberg FP, Bullard DC, Caver TE, Gresham HD, Beaudet AL, Brown EJ. 1996. Decreased resistance to bacterial infection and granulocyte defects in IAP-deficient mice. Science 274:795-8.
55. Azcutia V, Kelm M, Luissint AC, Boerner K, Flemming S, Quiros M, Newton G, Nusrat A, Luscinskas FW, Parkos CA. 2020. Neutrophil expressed CD47 regulates CD11b/CD18-dependent neutrophil transepithelial migration in the intestine in vivo. Mucosal Immunol doi:10.1038/s41385-020-0316-4.
56. Jaiswal S, Jamieson CH, Pang WW, Park CY, Chao MP, Majeti R, Traver D, van Rooijen N, Weissman IL. 2009. CD47 is upregulated on circulating hematopoietic stem cells and leukemia cells to avoid phagocytosis. Cell 138:271-85.
57. Zhang Z, Jin L, Champion G, Seydel KB, Stanley SL, Jr. 2001. Shigella infection in a SCID mouse-human intestinal xenograft model: role for neutrophils in containing bacterial dissemination in human intestine. Infect Immun 69:3240-7.
58. Staab JF, Lemme-Dumit JM, Latanich R, Pasetti MF, Zachos NC. 2020. Co-Culture System of Human Enteroids/Colonoids with Innate Immune Cells. Curr Protoc Immunol 131:e113.
59. Sato T, Stange DE, Ferrante M, Vries RG, Van Es JH, Van den Brink S, Van Houdt WJ, Pronk A, Van Gorp J, Siersema PD, Clevers H. 2011. Long-term expansion of epithelial organoids from human colon, adenoma, adenocarcinoma, and Barrett's epithelium. Gastroenterology 141:1762-72.
60. Parkos CA, Colgan SP, Delp C, Arnaout MA, Madara JL. 1992. Neutrophil migration across a cultured epithelial monolayer elicits a biphasic resistance response representing sequential effects on transcellular and paracellular pathways. J Cell Biol 117:757-64.
61. Brouwer N, Dolman KM, van Houdt M, Sta M, Roos D, Kuijpers TW. 2008. Mannose-binding lectin (MBL) facilitates opsonophagocytosis of yeasts but not of bacteria despite MBL binding. J Immunol 180:4124-32.
62. Chaka W, Scharringa J, Verheul AF, Verhoef J, Van Strijp AG, Hoepelman IM. 1995. Quantitative analysis of phagocytosis and killing of Cryptococcus neoformans by human peripheral blood mononuclear cells by flow cytometry. Clin Diagn Lab Immunol 2:753-9.

Figure legends

Figure 1. Establishment of a human PMN-enteroid co-culture. (**A**) May-Grünwald Giemsa image of PMN isolated from peripheral blood [left]. Representative dot plot of PMN phenotype [middle] and schematic representation the PMN-enteroid co-culture model [right]. (**B**) Confocal XZ projection [top; right, magnification XY projection] and H&E [bottom] images of the PMN-enteroid co-culture. Confocal: DNA, blue; actin, white; CD16 (PMN), green; Transwell insert, dashed lines. Arrowheads indicate PMN seeded on the Transwell insert and at the base of the columnar epithelium. (**C**) Representative immunofluorescence confocal microscopy image [top, XY; bottom, XZ projections] of the enteroid apical surface showing PMN intercalated and moving up within the epithelial cell monolayer. DNA, blue; CD16 (PMN), green; actin, white; Transwell insert, dashed line. (**D**) Number of PMN transmigrated to the luminal compartment 2h after being added to the co-culture in the absence or presence of apically delivered rhIL-8. (**E**) TER of enteroid monolayers and PMN-enteroid co-cultures in a 2h co-culture. (**F**) TER of enteroid monolayers and PMN-enteroid co-culture apically treated with rhIL-8 for 2h. (**G**) Total amount of cytokines secreted into the apical and basolateral compartments after 2h of co-culture. (D, E, F) Each dot represents the average from three replicate wells; data are shown as mean ± sem from 3 independent experiments. (G) Data are shown as mean + sem from 3 independent experiments in triplicate. *p* values were calculated by Student's *t*-test. See also Figure S1.

Figure 2. Distinctive phenotype of PMN within the human intestinal environment. (**A**) Schematic representation of PMN in direct contact with epithelial cells (C) or in the basolateral media (BM). (**B, C, D**) Phenotype of isolated PMN, PMN in C and BM determined by flow cytometry within 2h of co-culture. Each dot represents data collected from three replicate wells; data are shown as mean ± sem from 3 independent experiments. *p* values were calculated by one-way-ANOVA with Tukey's post-test for multiple comparisons. See also Figure S2.

Figure 3. Innate immune responses of human PMN to *S. flexneri*. (**A**) Representative confocal microscopy image and histogram of *S. flexneri* 2a-FITC uptake by human PMN. Confocal image [left, XY projection]. DNA, blue; actin, red; *S. flexneri* 2a, green. Histograms of PMN harboring *Shigella*-FITC [middle] and percentage of phagocytosis at 10, 30 and 60 min post infection [left]. Each dot represents the average from three replicates and PMN from 5 individual donors; data are shown as mean ± sem from 3 independent experiments. (**B**) Extracellular *S. flexneri* 2a colony forming units (CFU) in culture media following PMN exposure to *S. flexneri* 2a ($1x10^8$ CFU/ml) for 30 and 60 min; controls included *S. flexneri* 2a in culture media or in PMN-conditioned media without PMN. Each dot represents the average from three replicates and PMN from 6 individual donors; data are shown as mean ± sem from 3 independent experiments. (A, B) *p* values were calculated by one-way ANOVA with Tukey's post-test for multiple comparisons. (**C**) PMN viability in the presence and absence of *S. flexneri* 2a. Data represents the average from three replicates and PMN from 3 individual donors; data are shown as mean ± sem from 3 independent experiments. (**D**) PMN morphology before (0 min) and after (30 min) exposure to *S. flexneri* 2a. (**E**) Confocal microscopy image [XY projection] of NETs 30 min after exposure to *S. flexneri* 2a. DNA, blue; actin, red; *S. flexneri* 2a, green. (**F**) Immunofluorescence image showing *S. flexneri* 2a-FITC colocalization in PMN lysosome. Arrowheads indicate bacteria intracellularly and within the lysosome compartment. (**G**) Total amount of cytokines secreted in culture supernatant of PMN alone and PMN exposed to *S. flexneri* 2a for 2h. Data are shown as mean ± sem from 3 independent experiments in triplicate. (C, G) *p* values were calculated by Student's *t* test. (**H**) Principal component analysis (PCA) plot of *Shigella*-exposure PMN v. PMN monoculture. Variables analyzed: phagocytosis, bactericidal activity, viability, IL-1β, IL-6, IL-8, TNF-α, and MCP-1 variables.

Figure 4. Coordinated innate immune response to *Shigella* by human intestinal epithelial cells and PMN. (**A**) Numbers of PMN transmigrated to the apical compartment of enteroid monolayers exposed or not to *S. flexneri* 2a for 2h. (**B and C**) Confocal microscopy images [B: top, XY; bottom, XZ projections; right, magnification] of PMN-enteroid co-culture infected with *S. flexneri* 2a for 2h. PMN: CD16 (B, green), CD15 (C, red); *S. flexneri* 2a (B, red; C, green); actin, white; nuclei, blue. White arrowheads indicate *S. flexneri* 2a. (**D**) CFU in the apical and basolateral media of enteroid and PMN-enteroid co-cultures apically exposed to *S. flexneri* 2a for 2h. (**E**) TER of enteroid and PMN-enteroid co-cultures exposed to *S. flexneri* 2a for 2h. (**F**) Total amount of cytokines in the apical and basolateral media of PMN-enteroid co-cultures exposed or not to *S. flexneri* 2a for 2h. (A, D, E) Each dot represents the average from three replicate wells; data are shown as mean ± sem from 3 (A, E) and 5 (D) independent experiments. *p* values were calculated by Student's *t*-test. (F) Data are shown as mean ± sem from 3 independent experiments in triplicate. *p* values were calculated by Student's *t*-test.

Figure 5. Immune phenotype of PMN co-cultured with epithelial cells and exposed to *Shigella*. (**A, B, C**) Cell surface expression of CD15, CD16, CD11b, CD18, CD88, CD66b, CD47, and CD182 on PMN embedded in the enteroid monolayer (co-culture) exposed or not to *S. flexneri* 2a for 2h. Each dot represents data collected from three replicate wells; data are shown as mean ± sem from 3 independent experiments. *p* values were calculated by Student's *t*-test. See also Figure S3.

Figure 1

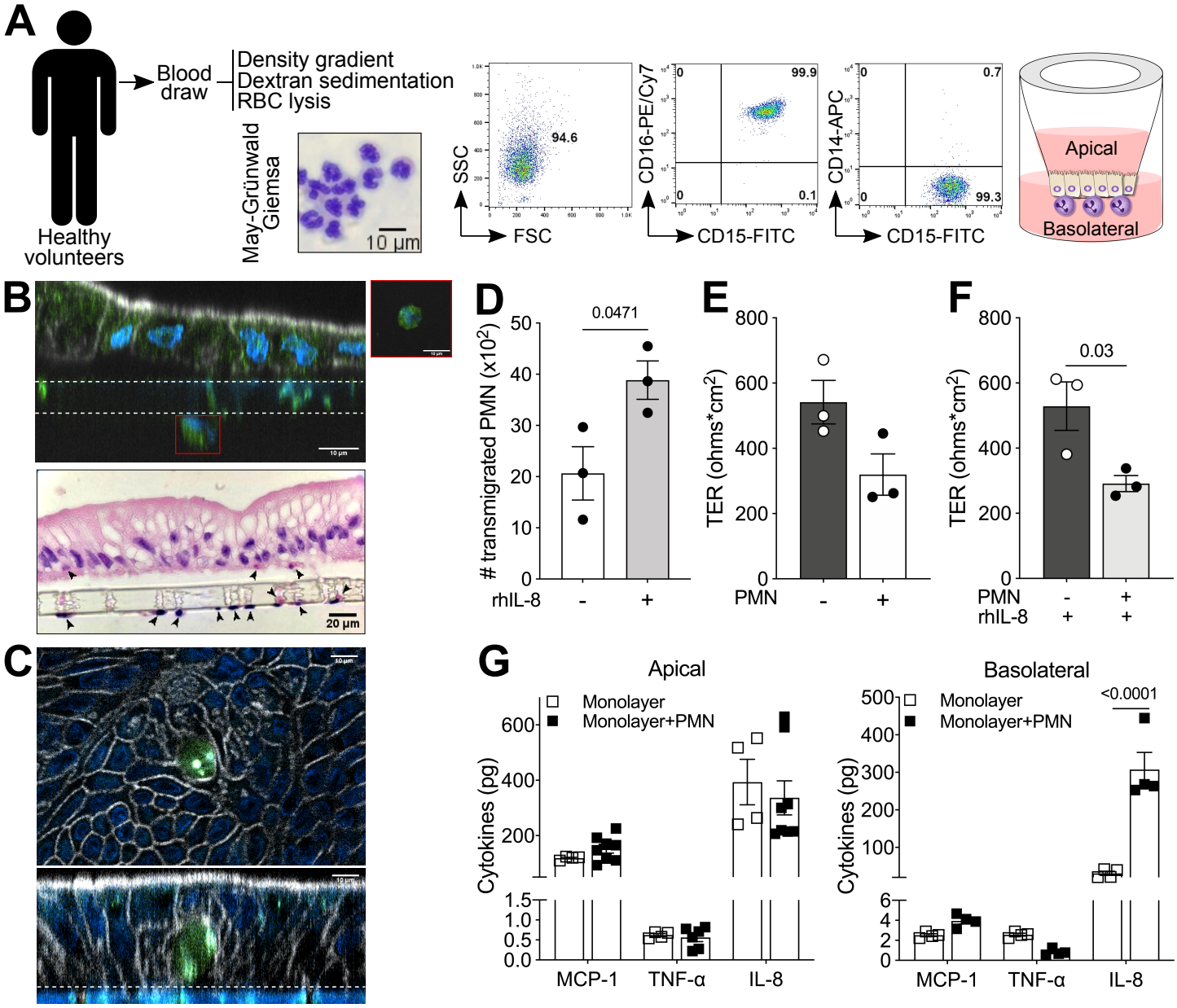
A
Healthy volunteers
Blood draw
Density gradient
Dextran sedimentation
RBC lysis
May-Grünwald Giemsa
10 µm
SSC
FSC
94.6
CD16-PE/Cy7
CD15-FITC
99.9
0.1
CD14-APC
CD15-FITC
0.7
99.3
Apical
Basolateral
B
10 µm
20 µm
C
D
transmigrated PMN (x10²)
0.0471
rhIL-8
E
TER (ohms*cm²)
PMN
F
TER (ohms*cm²)
0.03
PMN
rhIL-8
G
Apical
Basolateral
Monolayer
Monolayer+PMN
Cytokines (pg)
<0.0001
MCP-1
TNF-α
IL-8

Figure 2

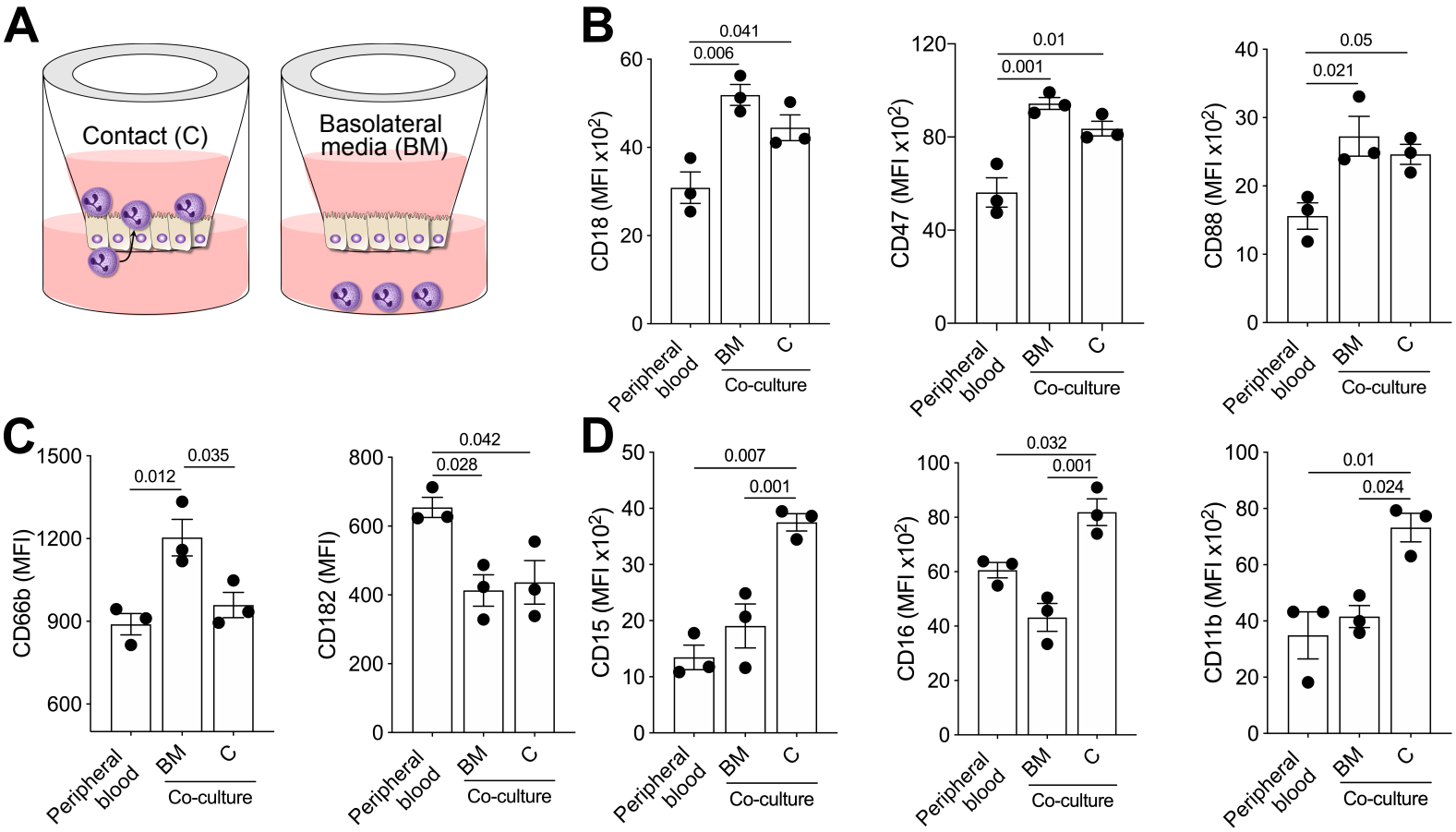
A
Contact (C)
Basolateral media (BM)
B
CD18 (MFI x10²)
0.041
0.006
CD47 (MFI x10²)
0.01
0.001
CD88 (MFI x10²)
0.05
0.021
C
CD66b (MFI)
0.012
0.035
CD182 (MFI)
0.042
0.028
D
CD15 (MFI x10²)
0.007
0.001
CD16 (MFI x10²)
0.032
0.001
CD11b (MFI x10²)
0.01
0.024
Peripheral blood
BM
C
Co-culture

Figure 3

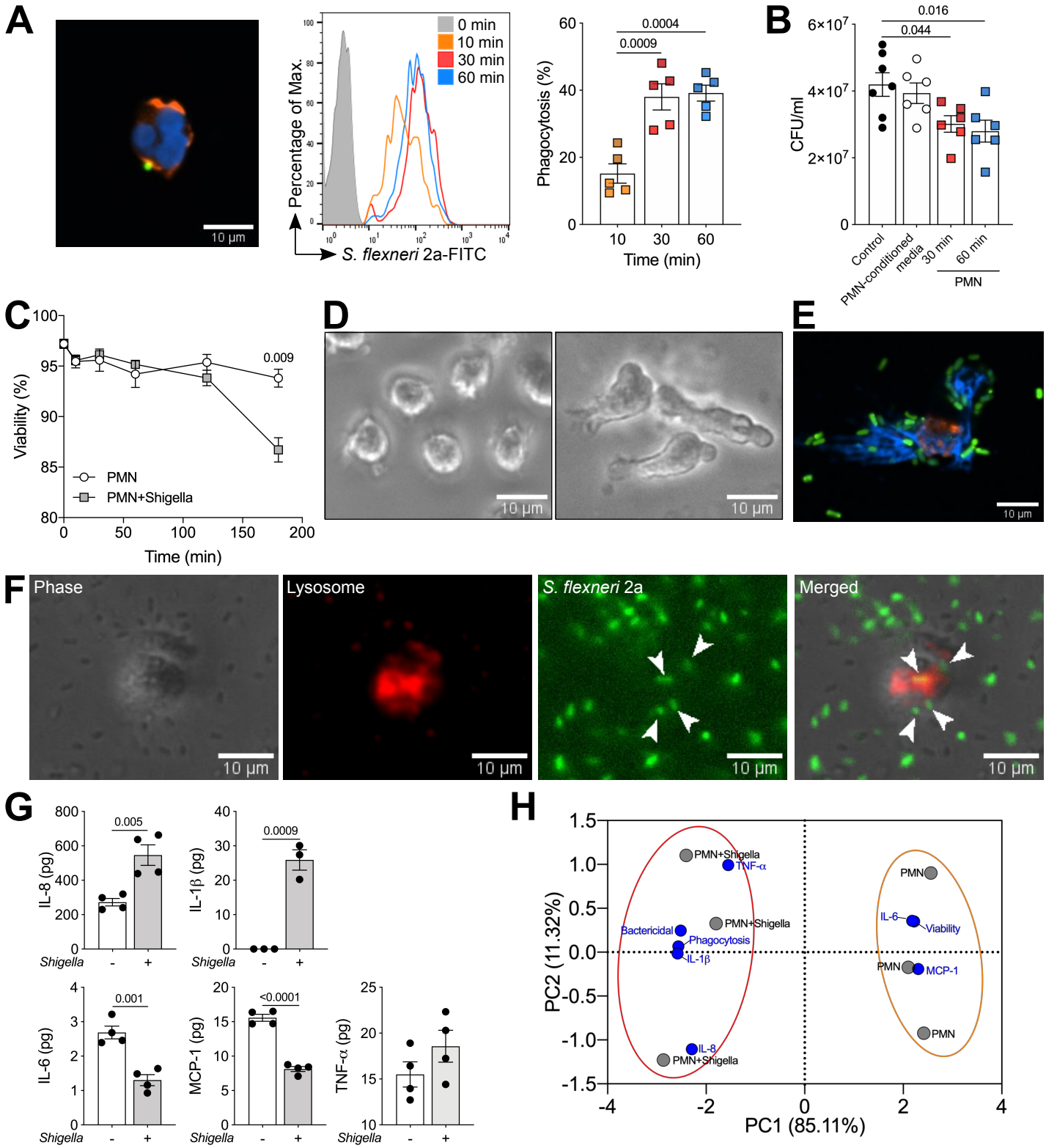
A
10 µm
0 min
10 min
30 min
60 min
Percentage of Max.
S. flexneri 2a-FITC
Phagocytosis (%)
0.0004
0.0009
Time (min)
B
0.016
0.044
CFU/ml
Control
PMN-conditioned media
30 min
60 min
PMN
C
Viability (%)
0.009
PMN
PMN+Shigella
Time (min)
D
10 µm
E
10 µm
F
Phase
Lysosome
S. flexneri 2a
Merged
10 µm
G
IL-8 (pg)
0.005
IL-1β (pg)
0.0009
IL-6 (pg)
0.001
MCP-1 (pg)
<0.0001
TNF-α (pg)
Shigella
H
PC2 (11.32%)
PC1 (85.11%)
PMN+Shigella
TNF-α
Bactericidal
Phagocytosis
IL-1β
IL-8
PMN
IL-6
Viability
MCP-1

Figure 4

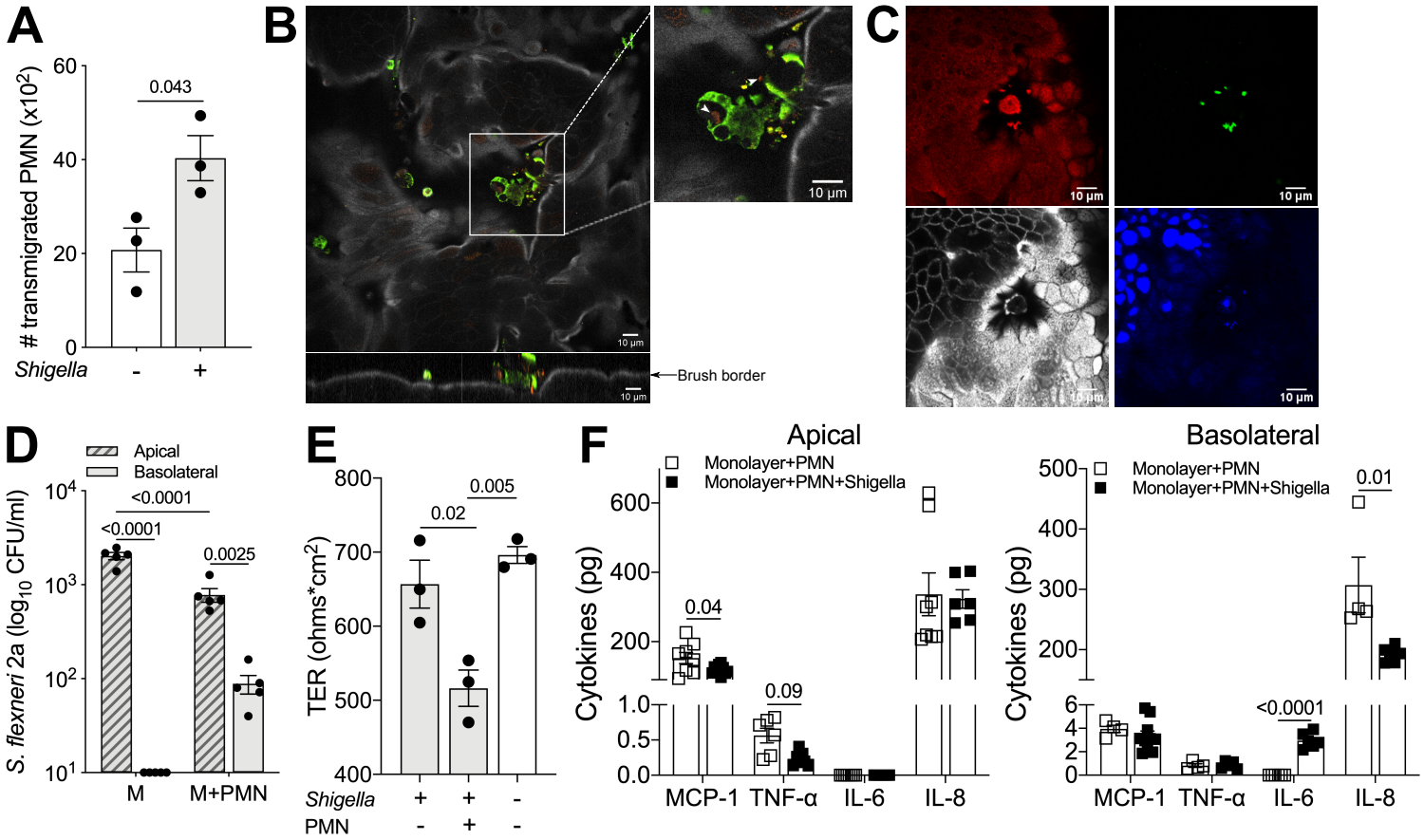
A
transmigrated PMN (x10^2)
60
40
20
0
0.043
Shigella
-
+
B
10 µm
Brush border
C
10 µm
D
Apical
Basolateral
S. flexneri 2a (log10 CFU/ml)
10^4
10^3
10^2
10^1
<0.0001
<0.0001
0.0025
M
M+PMN
E
TER (ohms*cm^2)
800
700
600
500
400
0.02
0.005
Shigella
PMN
F
Apical
Basolateral
Monolayer+PMN
Monolayer+PMN+Shigella
Cytokines (pg)
600
400
200
1.0
0.5
0.0
0.04
0.09
MCP-1
TNF-α
IL-6
IL-8
500
300
6
4
2
0
0.01
<0.0001

Figure 5

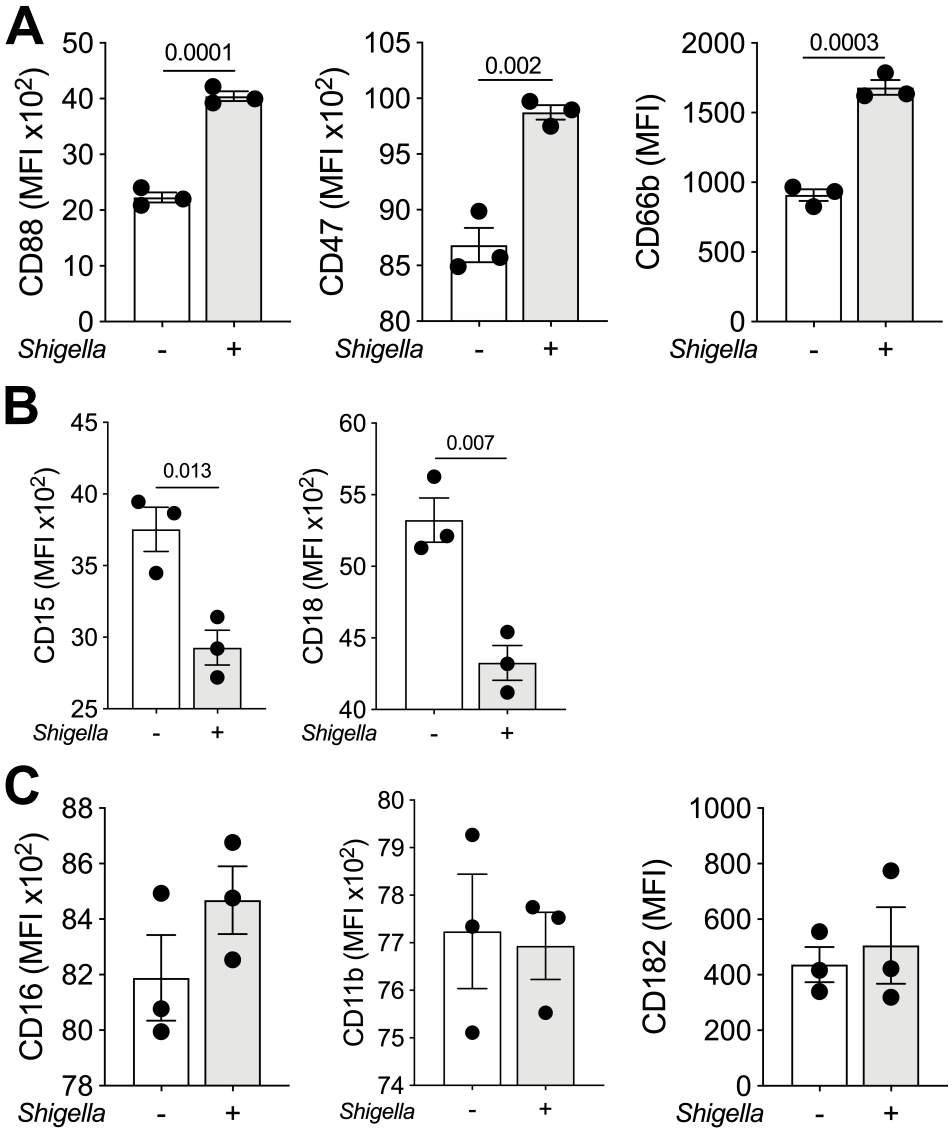
A
CD88 (MFI x10^2)
0.0001
CD47 (MFI x10^2)
0.002
CD66b (MFI)
0.0003
Shigella - +
B
CD15 (MFI x10^2)
0.013
CD18 (MFI x10^2)
0.007
Shigella - +
C
CD16 (MFI x10^2)
CD11b (MFI x10^2)
CD182 (MFI)
Shigella - +